Design of Functionally Graded Piezoelectric Actuators Using Topology Optimization

Ronny C. Carbonari[a], Emílio C. N. Silva[a], and Glaucio H. Paulino[b]

[a]Department of Mechatronics ad Mechanical Systems Engineering
Escola Politécnica da Universidade de São Paulo
Av. Prof. Mello Moraes, 2231, São Paulo - SP - 05508-900, Brazil
[b]Department of Civil and Environmental Engineering,
University of Illinois at Urbana-Champaign,
Newmark Laboratory, 205 North Mathews Av., Urbana, IL, 61801, USA

ABSTRACT

Functionally Graded Materials (FGMs) possess continuous variation of material properties and are characterized by spatially varying microstructures. Recently, the FGM concept has been explored in piezoelectric materials to improve properties and to increase the lifetime of bimorph piezoelectric actuators. Elastic, piezoelectric, and dielectric properties are graded along the thickness of a piezoceramic FGM. Thus, the gradation of piezoceramic properties can influence the performance of piezoactuators. In this work, topology optimization is applied to find the optimum gradation variation in piezoceramics in order to improve actuator performance measured in terms of output displacements. A bimorph type actuator design is investigated. The corresponding optimization problem is posed as finding the optimized gradation of piezoelectric properties that maximizes output displacement or output force at the tip of the bimorph actuator. The optimization algorithm combines the finite element method with sequential linear programming. The finite element method is based on the graded finite element concept where the properties change smoothly inside the element. This approach provides a continuum approximation of material distribution, which is appropriate to model FGMs. The present results consider gradation between two different piezoceramic properties and two-dimensional models with plane stress assumption.

Keywords: Micromachines, nanopositioners, piezoelectric actuators, topology optimization, finite element analysis

1. INTRODUCTION

Piezoelectric microdevices have a wide range of applications in precision mechanics, nanopositioning and micromanipulation fields. Functionally Graded Materials (FGMs) are advanced materials that possess continuously graded properties and are characterized by spatially varying microstructures created by nonuniform distributions of the reinforcement phase as well as by interchanging the role of reinforcement and matrix (base) materials in a continuous manner.[1] The smooth variation of properties may offer advantages such as local reduction of stress concentration and increased bonding strength. Recently, this concept has been explored in piezoelectric materials to improve properties and to increase the lifetime of bimorph piezoelectric actuators.[2] These actuators have attracted significant attention due to their simplicity and reliability. Usually, elastic, piezoelectric, and dielectric properties are graded along the thickness of an FGM bimorph piezoactuator. This gradation can be achieved by stacking piezoelectric composites of different compositions on top of each other.[3] Each lamina can be composed by a piezoelectric material or a composite made of piezoelectric material and a non-piezoelectric material. Many studies have been conducted on FGM bimorph actuators.[4–8] Previous studies[8] have shown that the gradation of piezoceramic properties can influence the performance of bimorph piezoactuators, such as

Further author information:
Ronny C. Carbonari: E-mail: ronny@usp.br, Telephone: +55 (11) 3091 9851
Emílio C. N. Silva: E-mail: ecnsilva@usp.br, Telephone: +55 (11) 3091 9754
Glaucio H. Paulino: E-mail: paulino@uiuc.edu, Telephone: +1 (217) 333 3817

Smart Structures and Materials 2006: Modeling, Signal Processing, and Control,
edited by Douglas K. Lindner, Proc. of SPIE Vol. 6166, 616607, (2006)
0277-786X/06/$15 · doi: 10.1117/12.658562

generated output displacements. *This suggests that optimization techniques can be applied to take advantage of the property gradation variation to improve FGM piezoactuators.*

Thus, in this work, *topology optimization is applied to find the optimum gradation variation in FGM piezoceramics to improve piezoactuator performance measured in terms of output displacements* (see Figure 1). A bimorph type actuator design is considered. Accordingly, the optimization problem is posed as finding the optimized gradation variation of piezoelectric properties that maximizes output displacement or output force at the tip of the bimorph actuator while minimizing the effects of movement coupling. The optimization algorithm combines the finite element method (FEM) with sequential linear programming (SLP). The FEM is based on the graded finite element concept where the material properties change smoothly inside the element. The material model is implemented based on the solid non-piezoelectric material with penalization (SIMP)[9] where fictitious densities are interpolated at each finite element. This approach provides a continuum approximation of material distribution (CAMD),[10] which is appropriate to model FGMs. The alternative FGM modelling using traditional FEM formulation and discretizing the FGM into layers gives a discontinuous stress distribution,[8] which is problematic.[11] The present results consider gradation between either two different piezoceramic properties or gold and piezoceramic properties, and consider two-dimensional models with plane stress assumption. Potentially, the practical use of the proposed approach can dramatically broaden the range of application of functionally graded piezoelectric actuators in the field of smart structures.

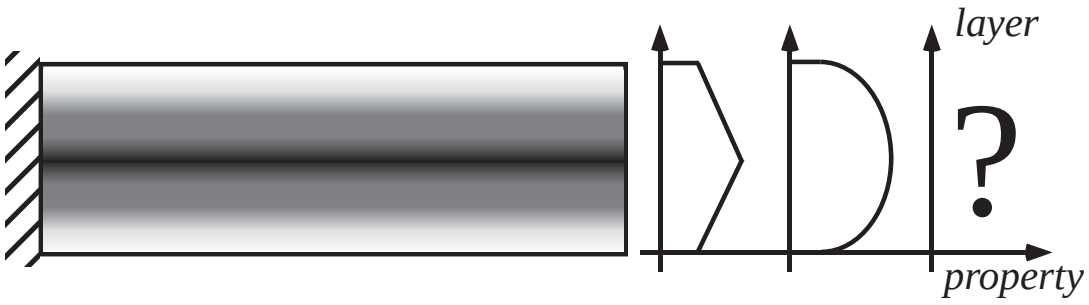

Figure 1. Finding the optimum gradation variation in piezoceramics FGMs.

2. FUNCTIONALLY GRADED PIEZOELECTRIC FINITE ELEMENT MODEL

In this work, FGM piezoelectric actuators considered for design operate in quasi-static or low-frequency (inertia effects are neglected). Thus the FEM matrix formulation of the equilibrium equations for the piezoelectric medium is given by[12]:

$$\begin{bmatrix} \mathbf{K_{uu}} & \mathbf{K_{u\phi}} \\ \mathbf{K}^t_{\mathbf{u}\phi} & -\mathbf{K}_{\phi\phi} \end{bmatrix} \begin{Bmatrix} \mathbf{U} \\ \mathbf{\Phi} \end{Bmatrix} = \begin{Bmatrix} \mathbf{F} \\ \mathbf{Q} \end{Bmatrix} \Longrightarrow [\mathcal{K}]\{\mathcal{U}\} = \{\mathcal{Q}\} \tag{1}$$

where $\mathbf{K_{uu}}$, $\mathbf{K_{u\phi}}$, and $\mathbf{K}_{\phi\phi}$ are the stiffness, piezoelectric, and dielectric matrices, respectively, and $\mathbf{F}$, $\mathbf{Q}$, $\mathbf{U}$, and $\mathbf{\Phi}$ are the nodal mechanical force, nodal electrical charge, nodal displacements, and nodal electric potential vectors, respectively.[12] The material properties continuously change inside the piezoceramic domain, which means that they can be described by some continuous function of position $(\mathbf{x})$ of the piezoceramic domain, that is:

$$\mathbf{c}^E = \mathbf{c}^E(\mathbf{x});\ \mathbf{e} = \mathbf{e}(\mathbf{x});\ \boldsymbol{\epsilon}^S = \boldsymbol{\epsilon}^S(\mathbf{x}) \tag{2}$$

where $\mathbf{c}^E$, $\mathbf{e}$, and $\boldsymbol{\epsilon}^S$ are the stiffness, piezoelectric and dielectric properties, respectively. As a consequence, according to the mathematical definition of $\mathbf{K_{uu}}$, $\mathbf{K_{u\phi}}$, and $\mathbf{K}_{\phi\phi}$, these material properties remain inside the matrices integrals and are integrated using the graded finite element concept[11] where properties are continuously interpolated inside each finite element based on property values at each finite element node. Approximation of

the continuous change of material properties by a stepwise function, where a property value is assigned for each finite element, results in undesirable discontinuity of the stress field.[11]

Because a non-piezoelectric conductor material and a piezoceramic material may be distributed in the piezoceramic domain, the electrode positions are not known "a priori", as discussed ahead. Thus, the electrical excitation will be given by an applied electric field.[13] In this case, all electrical degrees of freedom are prescribed in the FEM problem, and thus, Eq. (1) becomes:

$$\left[\begin{array}{cc} \mathbf{K_{uu}} & \mathbf{K_{u\phi}} \\ \mathbf{K}_{\mathbf{u}\phi}^{t} & -\mathbf{K}_{\phi\phi} \end{array}\right] \left\{\begin{array}{c} \mathbf{U} \\ \mathbf{\Phi} \end{array}\right\} = \left\{\begin{array}{c} \mathbf{F} \\ \mathbf{Q} \end{array}\right\} \Longrightarrow \left\{\begin{array}{l} [\mathbf{K_{uu}}]\{\mathbf{U}\} = \{\mathbf{F}\} - [\mathbf{K_{u\phi}}]\{\mathbf{\Phi}\} \\ \left[\mathbf{K}_{\mathbf{u}\phi}^{t}\right]\{\mathbf{U}\} = \{\mathbf{Q}\} + [\mathbf{K}_{\phi\phi}]\{\mathbf{\Phi}\} \end{array}\right. \tag{3}$$

where $\{\mathbf{\Phi}\}$ is prescribed. Thus, the mechanical and electrical problems are decoupled, and only the upper problem of Eq. (3) needs to be directly solved. In this case, the optimization problem is essentially based on the mechanical problem. As a consequence the dielectric properties will not influence the design.

3. TOPOLOGY OPTIMIZATION FORMULATION

Topology optimization is a powerful structural optimization technique that combines the FEM with an optimization algorithm to find the optimal material distribution inside a given domain (extended fixed domain), bounded by supports and applied loads, that contains the unknown structure.[9,14]

The basic topology optimization formulation used in this work follows the formulation described in detail by Carbonari *et al.*.[15] It is a continuous topology optimization formulation in which a continuous distribution of the design variable inside the finite element is interpolated using some continuous function. In this case, the design variables are defined for each element node instead of each finite element as usual. This formulation, known as CAMD ("Continuous Approximation of Material Distribution")[10] is robust and it is also fully compatible with the FGM concept and philosophy.[15]

We are interested in a continuous distribution of piezoelectric materials in the design domain, and thus, the following material model is proposed based on a simple extension of the well-known SIMP model[9]:

$$\mathbf{C}^{H} = \rho\mathbf{C_1} + (1-\rho)\,\mathbf{C_2} \tag{4}$$

$$\mathbf{e}^{H} = \rho\mathbf{e_1} + (1-\rho)\,\mathbf{e_2} \tag{5}$$

where ρ ($\rho = 1.0$ denotes piezoelectric material **type 1** and $\rho = 0.0$ denotes piezoelectric material **type 2**) are pseudo-density functions describing the amount of material at each point of the domain. The design variables can assume different values at each finite element node. $\mathbf{C}^H$ and $\mathbf{e}^H$ are stiffness and piezoelectric tensor properties, respectively, of the homogenized material. $\mathbf{C_1}$ and $\mathbf{e}_1$ are tensors related to the stiffness and piezoelectric properties for piezoelectric material **type 1**, respectively, and $\mathbf{C_2}$ and $\mathbf{e_2}$ are the corresponding properties for piezoelectric material **type 2**. These are the properties of basic materials that will be distributed in the piezoceramic domain to form the FGM piezocomposite. The dielectric properties are not considered because a constant electric field is applied to the design domain as electrical excitation. As explained in Section 4, this decouples the electrical and mechanical problems eliminating the influence of dielectric properties in the optimization problem. Eventually, the piezoelectric material **type 2** can be substituted by a non-piezoelectric material (elastic material, such as Aluminum, for example), and in this case $\mathbf{e_2} = \mathbf{0}$. For a discretized domain into finite elements Eqs. (4) and (5) are considered for each element node, and the material properties inside each finite element are given by a function $\rho = \rho(\mathbf{x})$, according to the CAMD concept. This formulation leads to a continuous distribution of material along the design domain which is ideal for the FGMs. Thus, by finding nodal values of the unknown ρ function, we obtain indirectly the optimum material distribution functions, described in Eq. (2).

The theoretical formulation for piezoelectric actuator design optimization using topology optimization was developed by Carbonari *et al.*[15] and it will be briefly presented here. It allows us to design a device that generates the maximum output displacement, considering a fixed piezoceramic domain. However, in this work,

the piezoceramic domain is not fixed and the piezoceramic electrodes are not known "a priori". Thus, to surround this problem an electric field is applied to the domain as electrical excitation. Essentially, the objective function is defined in terms of generated output displacements ($\mathbf{u}_1$) for a certain applied electric field to the design domain. The mean transduction ($L_2(\mathbf{u}_1, \phi_1)$) concept is related to the electromechanical conversion represented by the displacement generated in region $\Gamma_{\mathbf{t}_2}$ (see Figure 2) along a specified direction due to an input electrical excitation in the medium. The subscripts are related to the load cases described in Figure 2 in which $\mathbf{E}_i = -\nabla\phi_i$ denotes the electrical field associated with load case i. Thus, the larger $L_2(\mathbf{u}_1, \phi_1)$, the larger the displacement generated in this region in the traction $\mathbf{t}_2$ direction due to an applied electric field to the medium. Considering d_i and ϕ_i the electrical displacement and electrical potential, respectively, the mean transduction is defined by[16]:

$$L_2(\mathbf{u}_1, \phi_1) = \int_{\Gamma_{t_2}} \mathbf{t}_2 \mathbf{u}_1 \, d\Gamma + \int_{\Gamma_{d_2}} d_2 \phi_1 \, d\Gamma = \int_{\Gamma_{t_2}} \mathbf{t}_2 \mathbf{u}_1 \, d\Gamma \tag{6}$$

as $d_2 = 0$ in this problem. Therefore, the maximization of output displacement generated in a region $\Gamma_{\mathbf{t}_2}$ is obtained by maximizing the *mean transduction* quantity ($L_2(\mathbf{u}_1, \phi_1)$). The load cases considered for calculation of mean transduction are shown in instances (a1) and (a2) of Figure 2.

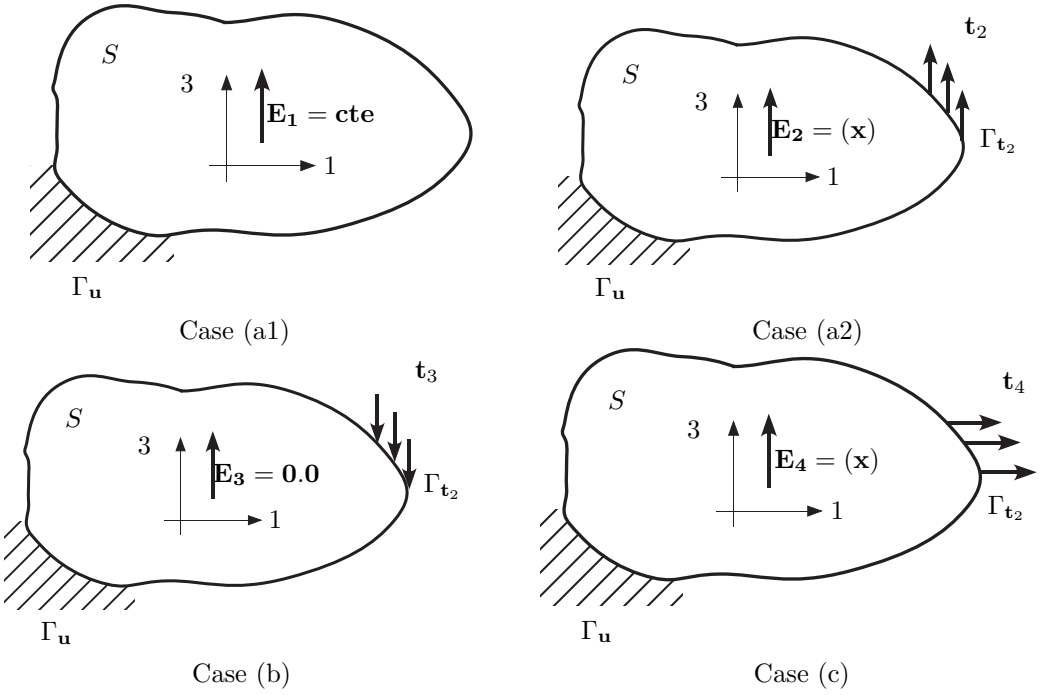

Figure 2. Load cases used for calculation of the mean transduction and coupling constraint (cases a1, a2, and c), and mean compliance (case b). Here, $\mathbf{E}_i = -\nabla\phi_i$ denotes the electrical field associated with load case i.

The piezoactuator must resist to reaction forces (in region $\Gamma_{\mathbf{t}_2}$) generated by a body that the piezoactuator is trying to move or grab. Therefore, the mean compliance must be minimized to provide enough stiffness (see Figure 2b). The mean compliance is calculated by considering the load case described in case (b) of Figure 2 where traction $\mathbf{t}_3 = -\mathbf{t}_2$ is applied to region $\Gamma_{\mathbf{t}_2}$, and the electric field is kept null inside the medium. Thus, the mean compliance is defined by[16]:

$$L_3(\mathbf{u}_3, \phi_3) = \int_{\Gamma_{t_2}} \mathbf{t}_3 \mathbf{u}_3 \, d\Gamma \tag{7}$$

The displacement coupling constraint is obtained by minimizing the absolute value of the corresponding mean transduction related to undesired generated displacement. This will minimize an undesired displacement generated when an electric field is applied. Therefore, the mean transduction $L_4(\mathbf{u}_1, \phi_1)$ related to the displacement normal to the desired displacement at $\Gamma_{\mathbf{t}_2}$ must be minimized (see Figure 2c), and it is calculated by using Eq. (6), however, considering a traction $\mathbf{t}_4$, normal to $\mathbf{t}_2$, on region $\Gamma_{\mathbf{t}_2}$ instead,[15] as described in case (c) of Figure 2.

To properly combine the mean transduction, mean compliance maximization, and coupling constraint minimization, a multi-objective function is constructed to find an appropriate optimal solution that can incorporate all design requirements. The following multi-objective function is proposed to combine all these optimization aspects:

$$\mathcal{F}(\rho) = w * \ln\left[L_2(\mathbf{u}_1, \phi_1)\right] - \frac{1}{2}(1-w)\ln\left[L_3(\mathbf{u}_3, \phi_3)^2 + \beta L_4(\mathbf{u}_1, \phi_1)^2\right] \tag{8}$$
$$0 \leq w \leq 1$$

where w is a weight coefficient ($0 \leq w \leq 1$). The coefficient w allows control of the contributions of mean transduction (Eq. 6), mean compliance (Eq. 7), and displacement coupling in the design. Accordingly, the final optimization problem is defined as:

$$\begin{array}{ll} Maximize: & \mathcal{F}(\rho) \\ \rho(\mathbf{x}) & \\ subject\ to: & \text{Equilibrium equations for different load cases} \\ & 0 \leq \rho(\mathbf{x}) \leq 1 \\ & \Theta(\rho) = \int_S \rho dS - \Theta_1 \leq 0 \end{array}$$

where S is the design domain, Θ is the volume of piezoceramic **type 1** material in the design domain, Θ_1 is the upper-bound volume constraint defined to limit the maximum amount of material **type 1**. The other constraints are equilibrium equations for the piezoelectric medium (see Section 2) considering different load cases. These equations are solved separately from the optimization problem. They are stated in the optimization problem to indicate that, whatever topology is obtained, it must satisfy this equilibrium equations. Our notation follows the work of Bendsøe and Kikuchi.[14]

4. NUMERICAL IMPLEMENTATION

In this work, the continuous distribution of design variable $\rho(\mathbf{x})$ is given by function[10, 17]

$$\rho(\mathbf{x}) = \sum_{I=1}^{n_d} \rho_I N_I(\mathbf{x}) \tag{9}$$

where ρ_I is a nodal design variable, N_I is the finite element shape function, and n_d is the number of nodes at each finite element. The design variable ρ_I can assume different values at each finite element node. Due to the definition of Eq. (9), the material property functions (Eqs. 4 and 5) will also have a continuous distribution inside the design domain. Thus, considering the mathematical definitions of the stiffness and piezoelectric matrices of Eq. (1), the material properties must remain inside the integrals and be integrated together by using the graded finite element concept.[11]

The FEM matrix formulation of equilibrium Eq. (1), the mean transduction (Eq. 6) and mean compliance (Eq. 7) can be calculated numerically through the expressions[16]:

$$\begin{aligned} L_2(\mathbf{U}_1, \mathbf{\Phi}_1) &= \{\mathbf{U}_1\}^t \{\mathbf{F}_2\} + \{\mathbf{\Phi}_1\}^t \{\mathbf{Q}_2\} = \{\mathbf{U}_1\}^t \{\mathbf{F}_2\} \\ &= \{\mathbf{U}_1\}^t [\mathbf{K}_{\mathbf{u}\phi}]_1 \{\mathbf{\Phi}_2\} - \{\mathbf{\Phi}_1\}^t [\mathbf{K}_{\phi\phi}]_1 \{\mathbf{\Phi}_2\} \end{aligned} \tag{10}$$

$$\begin{aligned} L_3(\mathbf{U}_3, \mathbf{\Phi}_3) &= \{\mathbf{U}_3\}^t \{\mathbf{F}_3\} + \{\mathbf{\Phi}_3\}^t \{\mathbf{Q}_3\} = \{\mathbf{U}_3\}^t \{\mathbf{F}_3\} \\ &= \{\mathbf{U}_3\}^t [\mathbf{K}_{\mathbf{uu}}]_3 \{\mathbf{U}_3\} + \{\mathbf{U}_3\}^t \left[\mathbf{K}^t_{\mathbf{u}\phi}\right]_3 \{\mathbf{\Phi}_3\} \end{aligned} \tag{11}$$

since $\{\mathbf{\Phi}_1\}^t \{\mathbf{Q}_2\} = 0$ (since $\{\mathbf{Q}_2\} = 0$) and $\{\mathbf{\Phi}_3\}^t \{\mathbf{Q}_3\} = 0$ (since $\{\mathbf{\Phi}_3\} = 0$). The expression for $L_4(\mathbf{U}_1, \mathbf{\Phi}_1)$ is equal to Eq. (10) substituting $\{\mathbf{F}_2\}$ by $\{\mathbf{F}_4\}$ and $\{\mathbf{Q}_2\}$ by $\{\mathbf{Q}_4\}$. The finite element equilibrium Eq. (1) is solved considering 4-node isoparametric finite elements under either plane stress or plane strain assumption.

A relevant problem to be solved is how to define the piezoceramic electrodes. In previous design optimization problems for piezoelectric actuators[15,16] the piezoceramic domain remains fixed and only the coupling structural domain (elastic material) is changed. Thus, the position of electrodes surface is known. However, if non-piezoelectric (such as Aluminum) and piezoelectric material are distributed in the design domain we cannot define a priori the position of the piezoceramic electrodes because we do not know where the piezoceramic is located in the design domain. To circunvent this problem, we consider the electrical problem independently for each finite element by defining a pair of electrodes at each finite element, that is, each finite element has its own electrical degrees of freedom, as described in Figure 3, in which u_i and v_i denote the node i horizontal and vertical displacement, respectively, and ϕ_{ij} denotes the j-th potential at the i-th node.

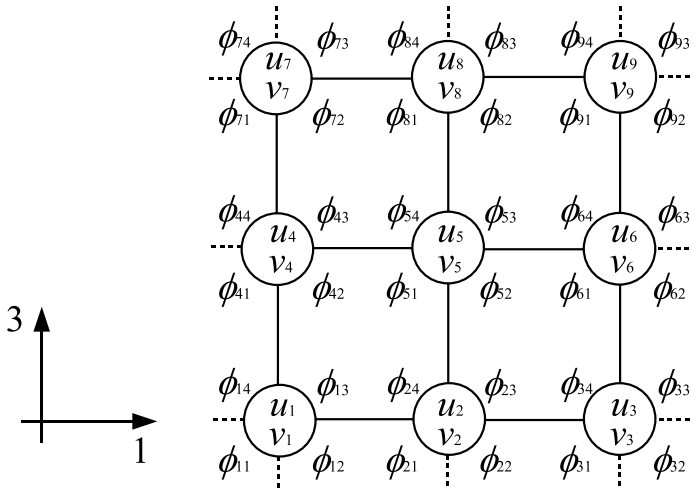

Figure 3. Finite elements with their corresponding electrical degrees of freedom. Here, u_i and v_i denote the node i horizontal and vertical displacement, respectively, and ϕ_{ij} denotes the j-th potential at the i-th node.

Thus, each finite element has 4 electrical degrees of freedom given by $[\phi_a, \phi_b, \phi_c, \phi_d]$ (nodes are ordered counterclockwise starting from the upper right corner of each finite element) considering that one of the electrodes is grounded. Electrical voltage ϕ_0 is applied to the two upper nodes, and thus, the four electrical degrees of freedom will be specified at each finite element ($[\phi_0, \phi_0, 0, 0]$).[13] This is equivalent to applying a constant electrical field along the 3-direction in the design domain (see Figure 3).

Thus, the discretized form of the final optimization problem is stated as:

$$
\begin{array}{lll}
\mathit{Maximize}: & \mathcal{F}(\rho_I) & \\
\rho_I & & \\
\mathit{subject\ to}: & \{\mathbf{F}_3\} = -\{\mathbf{F}_2\} \qquad (\Gamma_{\mathbf{t}_3} = \Gamma_{\mathbf{t}_2}) & \\
& \{\mathbf{F}_4\}^t \{\mathbf{F}_2\} = 0 \qquad (\Gamma_{\mathbf{t}_4} = \Gamma_{\mathbf{t}_2}) & \\
& [\mathcal{K}_1]\{\mathcal{U}_1\} = \{\mathcal{Q}_1\} & [\mathcal{K}_2]\{\mathcal{U}_2\} = \{\mathcal{Q}_2\} \\
& [\mathcal{K}_3]\{\mathcal{U}_3\} = \{\mathcal{Q}_3\} & [\mathcal{K}_2]\{\mathcal{U}_4\} = \{\mathcal{Q}_4\} \\
& 0 \le \rho_I \le 1 & I = 1..N_e \\
& \sum_{I=1}^{N_{des}} \rho_I V_I - \Theta_1 \le 0 &
\end{array}
$$

where V_I is the volume associated with each finite element node and is equal to finite element volume. N_{des} is the number of nodes in the design domain. $[\mathcal{K}_1]$ and $[\mathcal{K}_3]$ are reduced forms of matrix $[\mathcal{K}_2]$ considering non-zero

and zero prescribed voltage degrees of freedom in the domain, respectively. The initial domain is discretized by finite elements and the design variables are the values of ρ_I defined at each finite element node.

The boundary conditions for the piezoceramic domain for load cases (a1), (a2), (b), and (c) of Figure 2 are shown in Figures 4(a), (b), (c) and (d), respectively.

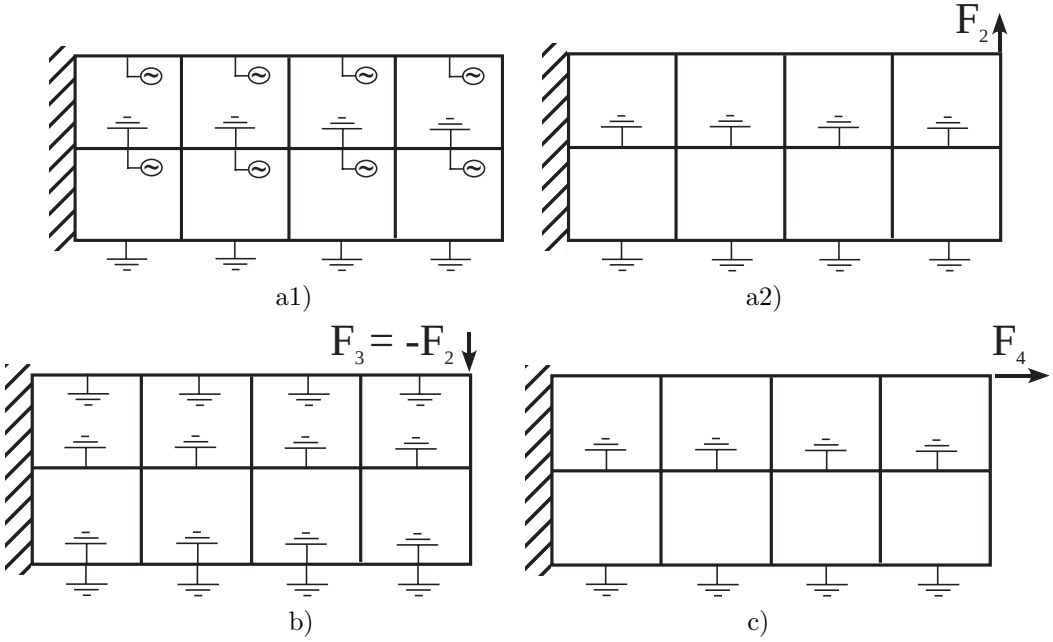

Figure 4. Electrical boundary conditions for the design domain: a1) and a2) mean transduction; b) mean compliance; c) coupling constraint function.

A flow chart of the optimization algorithm describing the steps involved is shown in Figure (5). The software was implemented using the C language.

The mathematical programming method called Sequential Linear Programming (SLP) is applied to solve the optimization problem since there are a large number of design variables, and different objective functions and some constraints are considered.[18, 19] The linearization of the problem (Taylor series) at each iteration requires the sensitivities (gradients) of the multi-objective function and constraints. These sensitivities will depend on gradients of mean transduction and mean compliance functions in relation to ρ_I.

Suitable moving limits are introduced to assure that the design variables do not change by more than 5–15% between consecutive iterations. A new set of design variables ρ_I are obtained after each iteration, and the optimization continues until convergence is achieved for the objective function.

5. RESULTS

The design of a bimorph piezoactuator will be presented to illustrate the FGM piezoelectric actuator design using the proposed method. The idea is to simultaneously distribute two types of piezoelectric material or a non-piezoelectric (in this case, Gold) and piezoelectric material. The design domain for this problem is shown in Figure 6 and it has 5500 finite elements (rectangle discretized by a 500×11 mesh). The bimorph is essentialy a piezoelectic cantilever type actuator. The design domain is divided into 11 horizontal layers and a design variable (pseudo density ρ_I) is considered for each layer interface, as described in Figure 8. Thus, there are 12 design variables. The center layer is made of Gold and it is kept fixed during optimization (non-optimized region). The mechanical and electrical boundary conditions are shown in the same figure.

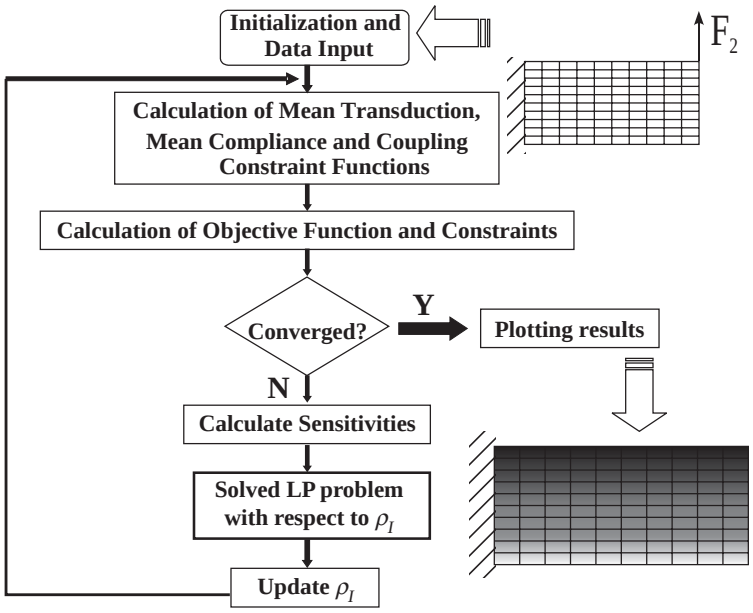

Figure 5. Flow chart of optimization procedure.

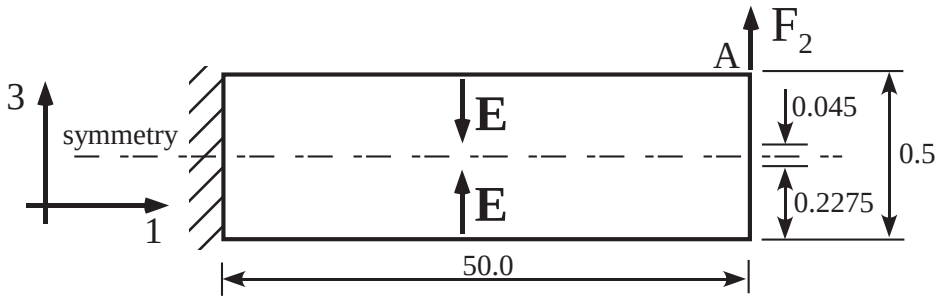

Figure 6. Bimorph design domain.

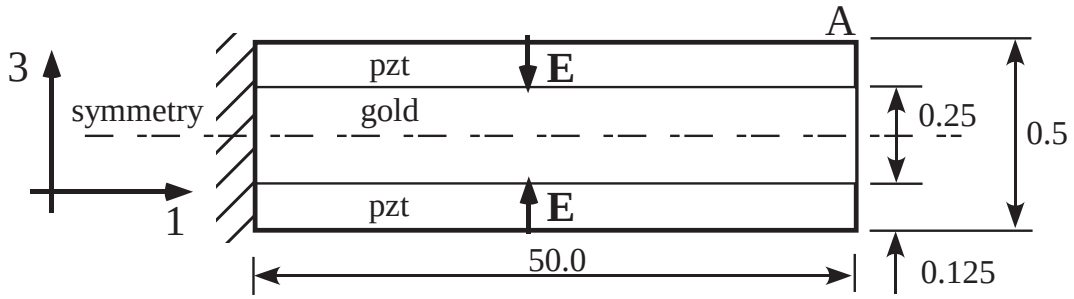

Figure 7. Standard bimorph.

Table (1) presents the piezoelectric material properties used in the simulations for all examples. $\mathbf{c}^E$ and $\mathbf{e}$ are the elastic and piezoelectric properties, respectively, of the medium. The Young's modulus and Poisson's ratio of Gold are equal to 83 GPa and 0.44, respectively. Two-dimensional isoparametric finite elements under plane-stress assumption are used in the finite element analysis.

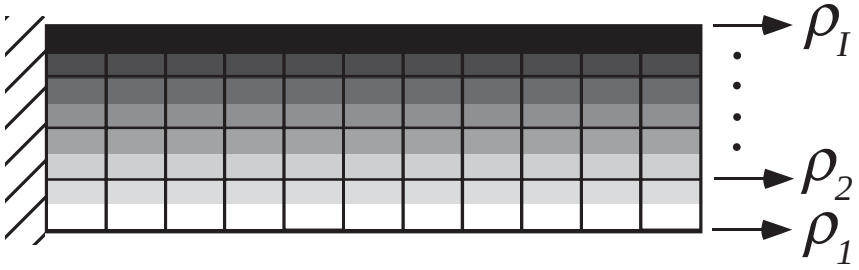

Figure 8. Bimorph design domain divided in horizontal layers. A design variable is defined for each layer interface.

Table 1. Material Properties of PZT5A.

c_{11}^E (10^{10} N/m^2)	12.1	e_{13} (C/m^2)	-5.4
c_{12}^E (10^{10} N/m^2)	7.54	e_{33} (C/m^2)	15.8
c_{13}^E (10^{10} N/m^2)	7.52	e_{15} (C/m^2)	12.3
c_{33}^E (10^{10} N/m^2)	11.1		
c_{44}^E (10^{10} N/m^2)	2.30		
c_{66}^E (10^{10} N/m^2)	2.10		

The electric field applied to the design domain is equal to 2200 V/mm (see Figure 6). Two designs were obtained considering the value of w coefficient equal to 0.5 and 1.0, respectively. The displacement coupling constraint was not activated, thus, the coefficient β is equal to zero in both cases. The volume constraint for piezoelectric material Θ_1 is set equal to 50%. The initial value for design variables (ρ_I) is equal to 0.15 in both cases. Thus, the optimization problem starts in the feasible domain (all constraints satisfied). The results are shown by plotting the pseudo-density gradation variation along the layers. Through material models described in Eqs. (4) and (5) the property gradation variation can be obtained. The topology optimization results are shown in Figure 9.

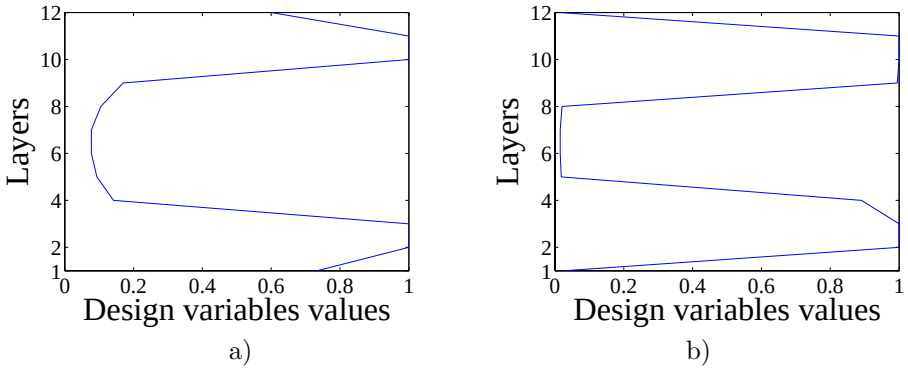

Figure 9. Bimorph optimal topology designs; a) $w = 0.5$; b) $w = 1.0$.

The optimization algorithm concentrates the piezoceramic in the upper and lower layers of the design domain. The property gradation variation is symmetric in both cases. The optimization finished with the constraint Θ_1 active in both designs. Table 2 describes X and Y displacement (u_x and u_y) at point A (see Figure 6) considering $2200V/mm$ electric field applied to the piezoceramic and coupling factors ($R_{yx} = u_x/u_y$) for obtained bimorph designs. Notice the weak coupling between horizontal and vertical displacements.

Table 2. Vertical displacement at point A ($2200V/mm$ applied) and coupling factor (R_{yx}).

Bimorph	$u_x(mm)$	$u_y(mm)$	$R_{yx}(\%)$	w	β	Θ_1
Fig.9a	2.02	-0.02	0.99	0.5	0.0	0.5
Fig.9b	2.11	-0.02	0.95	1.0	0.0	0.5
Fig.7	2.02	-0.02	0.99	-	-	0.5

From Table 2, comparing with the output displacement generated by the standard bimorph, the result from Figure 9b presented some improvement. The low improvements are due to the fact Gold is very stiff in relation to piezoceramic. A design considering a second material with stiffness 10 times lower than piezoceramic will be considered in a next paper.

6. CONCLUSIONS

A topology optimization formulation was proposed which allows the search for an optimal gradation of piezoelectric material properties in the design of FGM piezoelectric actuators, to achieve certain specified actuation movement. The optimization problem allows the simultaneous distribution of two piezoelectric materials or a non-piezoelectric (such as Gold) and piezoelectric materials in the design domain. In addition, a displacement coupling constraint that minimizes undesired actuated displacements is also considered in the design. The adopted material model in the formulation is based on the density method and it interpolates fictitious densities at each finite element based on pseudo-densities defined as design variables for each finite element node providing a continuous material distribution in the domain. The design of an FGM bimorph actuator is presented to illustrate that the actuator performance can be improved by finding the optimal gradation of FGM piezoelectric material properties in the actuator. Considering the maximization of output displacement, the optimization algorithm comes up with an optimized gradation variation of properties which consists of a distribution of piezoceramic material in the upper and lower layers and gold in the central layers.

Other performance criterias can be considered and other FGM piezoactuators can be optimized using the proposed approach help broadening the range of application of functionally graded piezoelectric actuators in the field of smart structures.

Acknowledgements

The first and second authors thank University of São Paulo (Brazil) and Fundação de Amparo à Pesquisa do Estado de São Paulo (FAPESP - Research Support Foundation of São Paulo State) for supporting them through a research project. The first author thanks the CNPq - Conselho Nacional de Desenvolvimento Científico e Tecnológico - Brazil, for supporting him through a doctoral fellowship ($n.^o 140687/2003-3$).

REFERENCES

1. S. Suresh and A. Mortensen, *Fundamentals of Functionally Graded Materials*, IOM Communications Ltd., London, England, 1988.
2. J. Ballato, R. Schwartz, and A. Ballato, "Network formalism for modeling functionally graded piezoelectric plates and stacks," *IEEE Transactions on Ultrasonics, Ferroelectrics and Frequency Control* **48**, pp. 462–476, 2001.
3. J. Qiu, J. Tani, T. Ueno, T. Morita, H. Takahashi, and H. Du, "Fabrication and high durability of functionally graded piezoelectric bending actuators," *Smart materials and Structures* **12**(1), pp. 115–121, 2003.
4. S. Zhifei, "General solution of a density functionally gradient piezoelectric cantilever and its applications," *Smart materials and Structures* **11**, pp. 122–129, 2002.
5. C. Ying and S. Zhifei, "Exact solutions of functionally gradient piezothermoelastic cantilevers and parameter identification," *Journal of Intelligent Material Systems and Structures* **16**, pp. 531–539, 2005.
6. E. Elka, D. Elata, and H. Abramovich, "The electromechanical response of multilayered piezoelectric structures," *Journal of Microelectromechanical Systems* **13**(42), pp. 332–341, 2004.

7. Z. F. Shi and Y. Chen, "Functionally graded piezoelectric cantilever beam under load," *Archive of Applied Mechanics* **74**, pp. 237–247, 2004.
8. A. Almajid, M. Taya, and S. Hudnut, "Analysis of out-of-plane displacement and stress field in a piezocomposite plate with functionally graded microstructure," *International Journal of Solids and Structures* **38**(19), pp. 3377–3391, 2001.
9. M. P. Bendsøe and O. Sigmund, *Topology Optimization - Theory, Methods and Applications*, Springer, New York, EUA, 2003.
10. K. Matsui and K. Terada, "Continuous approximation of material distribution for topology optimization," *International Journal for Numerical Methods in Engineering* **59**(14), pp. 1925–1944, 2004.
11. J. H. Kim and G. H. Paulino, "Isoparametric graded finite elements for nonhomogeneous isotropic and orthotropic materials," *ASME Journal of Applied Mechanics* **69**(4), pp. 502–514, 2002.
12. M. Naillon, R. H. Coursant, and F. Besnier, "Analysis of piezoelectric structures by a finite element method," *Acta Eletronica* **25(4)**, pp. 341–362, 1983.
13. M. J. Buehler, B. Bettig, and G. G. Parker, "Topology optimization of smart structures using a homogenization approach," *Journal of Intelligent Material Systems and Structures* **15**(8), pp. 655–667, 2004.
14. M. P. Bendsøe and N. Kikuchi, "Generating optimal topologies in structural design using a homogenization method," *Computer Methods in Applied Mechanics and Engineering* **71**, pp. 197–224, 1988.
15. R. C. Carbonari, E. C. N. Silva, and S. Nishiwaki, "Design of piezoelectric multiactuated microtools using topology optimization," *Smart Materials and Structures* **14**, pp. 1431–1447, 2005.
16. E. C. N. Silva, S. Nishiwaki, and N. Kikuchi, "Topology optimization design of flextensional actuators," *IEEE Transactions on Ultrasonics, Ferroelectrics and Frequency Control* **47**(3), pp. 657–671, 2000.
17. S. Rahmatalla and C. C. Swan, "A q4/q4 continuum structural topology optimization implementation," *Structural and Multidisciplinary Optimization* **27**, pp. 130–135, 2004.
18. G. N. Vanderplaatz, *Numerical Optimization Techniques for Engineering Design: with Applications*, McGraw-Hill, New York, USA, 1984.
19. R. Hanson and K. Hiebert, *A Sparse Linear Programming Subprogram*, Sandia National Laboratories, Technical Report SAND81-0297, 1981.